Multi-dimensional oscillatory activity of mouse GnRH neurons in vivo

Su Young Han[1], Shel-Hwa Yeo[1], Jae-Chang Kim[2], Ziyue Zhou[1] and Allan E. Herbison[1]

[1]Department of Physiology, Development and Neuroscience, Downing site, University of Cambridge, Cambridge CB2 3EG, UK and [2]Zurich Center for Neuroeconomics, Department of Economics, University of Zurich, 8006 Zurich, Switzerland

Corresponding author: Prof. Allan Herbison aeh36@cam.ac.uk

Disclosures: The authors have nothing to disclose and no competing interests.

Abstract

The gonadotropin-releasing hormone (GnRH) neurons represent the key output cells of the neural network controlling mammalian fertility. We used GCaMP fiber photometry to record the population activity of the GnRH neuron distal projections in the ventral arcuate nucleus where they merge before entering the median eminence to release GnRH into the portal vasculature. Recordings in freely behaving intact male and female mice revealed abrupt 5-min duration increases in activity that correlated perfectly with the appearance of a subsequent pulse of luteinizing hormone (LH). In addition, GnRH neuron dendrons exhibited a low level of clustered, rapidly fluctuating baseline activity in both sexes that did not change through the estrous cycle. In female mice, a gradual increase in basal activity that exhibited ~80-min oscillations began in the afternoon of proestrus and lasted for 12 h. This was associated with the onset of the LH surge that ended several hours before the fall in GCaMP signal. Abrupt episodes of GCaMP activity continued to occur on top of the rising surge baseline before ceasing in estrus. These observations provide the first description of GnRH neuron activity in freely behaving animals. They demonstrate three distinct patterns of oscillatory activity occur in GnRH neurons. These are comprised of low-level rapid baseline activity, abrupt short-duration oscillations that drive pulsatile gonadotropin secretion and, in females, a gradual and prolonged oscillating increase in activity responsible for the relatively short-lived preovulatory LH surge.

Introduction

The founding concepts of reproductive neuroendocrinology arose from the recognition by Harris and colleagues of the neurohumoral basis of the hypophyseal pituitary system (Harris 1955, Fink 2015) and the subsequent discovery by Schally and Guillemin and co-workers of the decapeptide gonadotropin-releasing hormone (GnRH) (Amoss, Burges et al. 1971, Schally, Arimura et al. 1971). This was soon followed by an appreciation that GnRH neurons had a very unusual topography in which cell bodies scattered throughout the basal forebrain sent projections to converge on the median eminence to release GnRH into the portal system (Barry 1979). The quest to understand the patterns of GnRH released into the portal system were largely solved by the portal bleeding approach in sheep (Clarke and Cummins 1982, Caraty and Locatelli 1988). Notably, this revealed that abrupt increments of GnRH secretion evoked pulsatile gonadotropin secretion whereas, in females, prolonged increases in constant or episodic GnRH secretion were responsible the preovulatory luteinizing hormone (LH) surge (Karsch, Bowen et al. 1997, Clarke 2018).

Establishing the activity patterns of GnRH neurons *in vivo* has been hampered considerably by their widely dispersed topography and, five decades on, remains an elusive goal (Herbison 2015, Constantin 2017). The development of transgenic GnRH-GFP mouse lines greatly facilitated efforts to record the electrical properties of individual GnRH neurons in the acute brain slice (Constantin, Moenter et al. 2021). However, the patterns of firing exhibited by GnRH neurons under these conditions have not been found to align well with predicted pulse or surge patterns of GnRH secretion (Herbison 2015, Constantin, Moenter et al. 2021). Similarly, the only report of GnRH neuron firing *in vivo* to date described a range of irregular firing patterns inconsistent with known hormone secretion (Constantin, Iremonger et al. 2013).

The episodic pattern of GnRH secretion driving pulsatile LH release is generated by the intermittent synchronised activity of the arcuate kisspeptin neuron population that projects to and controls the distal processes of GnRH neurons (Herbison 2018, Goodman, Herbison et al. 2022). These processes, termed dendrons in rodents, converge in the ventrolateral aspects of the arcuate nucleus (ARN) before turning into short axons that run into the median eminence (Herbison 2021). The GnRH neuron dendron appears to operate both as an autonomous site for GnRH pulse secretion while also carrying action potentials driving the GnRH surge that are initiated upstream at the level of the GnRH neuron cell bodies (Herbison 2020).

We have previously documented that the expression of GCaMP in GnRH neuron cell bodies and dendrons can be used to faithfully record GnRH neuron electrical activity *in vitro* (Iremonger, Porteous et al. 2017). As the ventrolateral ARN provides a unique location of concentrated GnRH neuron dendrons, we reasoned that it may be possible to record their activity in freely behaving mice at this location using GCaMP fiber photometry. We now demonstrate that this is indeed

possible and describe here the patterns of GnRH neuron activity underlying episodic and surge patterns of hormone secretion in male and female mice.

Results

Characterization of Gnrh1-GCaMP mouse

The Gnrh1-Cre mouse line (JAX stock #021207) (Yoon, Enquist et al. 2005) was crossed with the Ai162 (TIT2L-GC6s-ICL-tTA2)-D Cre-dependent GCaMP6s line (JAX stock #031562) (Daigle, Madisen et al. 2018) to generate Gnrh1-GCaMP6 mice. Dual immunofluorescence in four female mice demonstrated that 90±2% of GnRH neuron cell bodies expressed GCaMP within the rostral preoptic area (Fig.1A) as did the majority of GnRH dendrons and fibers within the ME (Fig.1B). In successfully recorded mice, optic fibers were found to be located immediately above or within the mid-caudal ARN (Fig.1C). Mice with unsuccessful recordings (n=4), that displayed no variation in GCaMP signal over 24h recordings, were found to have optic fibers located either mostly within the third ventricle or >200μM lateral to the ARN.

GnRH neuron activity in male mice

The GnRH neuron population activity at the level of distal dendron was measured for 24h starting between 10.00-11.00am in freely behaving Gnrh1-GCaMP6 male mice (n=7). Mice exhibited intermittent, abrupt increases in GCaMP signal termed here “dendron-synchronization episodes” (dSEs; Fig.2A). These episodes had a total duration of 658±5 s comprised of a rapid increase (full width at half maximum (FWHM) value of 30±4 s) and a slower decline (FWHM 102±7 s) (Fig.2C). The dSEs occurred on average every 93.3±7.4 min but had a large inter-interval range of 3.9 to 346.6 min and showed no clear modal distribution pattern (Fig.2D). The 24-h recordings also revealed another low amplitude, higher frequency baseline pattern activity (Fig.2A). Control recordings from mice with misplacement of fibers exhibited almost no baseline activity (Fig.2B).

The characteristics of dSEs strongly resembled those exhibited by arcuate nucleus kisspeptin neurons that drive pulsatile luteinizing hormone (LH) secretion (Han et al., 2019). Therefore, we assessed the relationship of GnRH neuron dSEs to LH pulses by taking 5- to 10-minute tail-tip blood samples for up to 240-min period while monitoring GCaMP fluorescence. This showed a perfect association between dSE occurrence and LH pulses (Fig.2E). Analysis of the temporal relationship between dSEs and LH pulses revealed that the peak of dSE consistently preceded LH pulses by 5.0±0.9 min (N=6 episodes in 5 mice; Fig.2F).

112
113
114 ***GnRH neuron activity in female mice***
115
116 To examine patterns of GnRH neuron activity across the estrous cycle, female Gnrh1-GCaMP6
117 mice were recorded for 6 h periods between 10am-4pm on each day of the cycle determined by
118 vaginal cytology on the morning of the recording. Similar to males, freely behaving female mice
119 exhibited a variable baseline pattern of high-frequency activity upon which intermittent, abrupt
120 increases in GCaMP signal occurred (Fig.3A). Each dSE showed a total duration of 463±22 s with
121 a rapid increase (FWHM 31±3 s) and a slower decline (FWHM 81±6 s) (Fig.3B). The frequency of
122 dSEs varied across the cycle in the same manner as kisspeptin neuron SEs (McQuillan, Han et al.
123 2019) with a dramatic slowing during estrus (dSE interval of 151.0±35.3 min; P=0.01 vs diestrus
124 and 0.001 vs proestrus, Dunn's posthoc; n=5) (Fig.3C). The inter-dSE intervals for metestrus,
125 diestrus and proestrus were not significantly different with mean±SEM of 70.2±6.7 min (n=8),
126 46.2±4.2 min (n=8), and 38.8±3.4 min (n=6), respectively (Fig.3C). Unlike in males, the overall
127 inter-dSE interval in females showed a clear right-skewed modal distribution with the inter-dSE
128 interval of 20 min being the most frequent mode (Fig.3D).
129
130 To examine the relationship of dSEs to LH pulses, tail-tip blood sampling was performed and
131 dSEs found to have a perfect correlation with LH pulses wherein the peak of a dSE occurred
132 6.1±0.2 min (N=6 episodes in 4 mice) before the peak of the following LH pulse (Fig.3E,F).

133
134 ***Low amplitude, clustered baseline activity in GnRH neurons in both male and female mice***
135
136 A low-amplitude, high-frequency GCaMP signal was observed in both male and female mice
137 (Fig.2A, 3A, 4A,B). This activity occurred in a cluster-like manner with mean cluster durations of
138 22.5±2.8 min (males), 30.0±3.9 min (metestrus), 31.9±6.7 min (diestrus) 24.8±2.2 min
139 (proestrus) and 35.3±6.8 min (estrus) in female mice. The intra-cluster frequency (range of
140 0.006-0.018 Hz) was not different between males and females (Fig.4D). Neither the mean
141 duration nor intra-cluster frequency of the baseline activity were different between males and
142 females or across the estrous cycle (Fig.4C,D). The amplitude of baseline signal was 10-12%
143 (males) and 5-12% (females) of the mean amplitude of dSEs.

144
145 ***GnRH neuron activity in proestrous female mice***
146
147 To examine patterns of GnRH neuron activity at the time of the preovulatory surge, female
148 Gnrh1-GCaMP6 mice (n=7) were recorded for a 24-hour period beginning on the morning of
149 proestrus. Initially, the signals were identical to those observed on metestrus and diestrus with a
150 low level of irregular baseline activity upon which abrupt, short increases in activity occurred

151 (Fig.3A,5A). A gradual increase in baseline activity was observed to begin 4.0±0.5 h (range 2-6.5
152 h) before "lights-off" (19:00h, 12:12 lighting) that peaked 5.9±0.5 h later and declined to
153 baseline by 12.6±0.8 h (range: 10.3-15.0 h)(Fig.5A). The FWHM period of incline and decline of
154 this slow activity was 3.1±0.4 and 4.7±0.5 h respectively, confirming the slow dynamics of the
155 signal. The slow increment in calcium signal was not smooth but consisted of multiple slow
156 oscillations (Fig.5A). The mean duration of these slow oscillations was 78±4 min (range 32 to 150
157 min). In addition, dSEs were observed to occur superimposed upon the slow oscillating signal
158 until around the time of peak baseline increment at which time they stopped for several hours
159 (Fig5A). Similar duration 24-hour recordings from metestrus-diestrous female mice found only
160 dSEs without any baseline shifts.
161
162 To assess the relationship of the slow oscillating signal to the LH surge, tail-tip bleeding with a 3-
163 hour interval was undertaken (Fig.5B). This showed that the LH surge began at the time of
164 baseline GCaMP change and peaked at 9.3±2.8 ng/ml close to when baseline GCaMP level was
165 at its highest ($\Delta F/F$ of 20-40%) (n=4). Notably, GCaMP activity greatly outlasted the duration of
166 the LH surge (Fig.5B).

167 To clarify the different components of GCaMP activity occurring on proestrus, we used a
168 customized Matlab code to separate out the three signals occurring at this time (Fig.6). Firstly, a
169 30-min rolling average was used to extract the slow oscillatory rise and decline in GCaMP
170 activity (Fig.6ii). The subtraction of this 'surge signal' from the original signal (Fig.6A) shows the
171 stereotypical dSEs and baseline fluctuations more clearly (Fig.6iii). Next, the peaks of individual
172 dSEs were selected and the signals from 60 s before and 360 s after each peak of dSE were
173 extracted. The remaining signals are considered to be 'the residual signal' comprising the high-
174 frequency basal activity described above (Fig.6iv).

175

176 **Discussion**

177 We reveal here three distinct oscillatory patterns of GnRH neuron activity in freely behaving
178 male and female mice. This includes a baseline of variable high-frequency cluster-like activity
179 upon which short abrupt episodes occur in both males and females and a prolonged, slowly
180 oscillating rise in activity on proestrus evening in females. These patterns of GnRH neuron
181 activity are sufficient to explain the pulse and surge patterns of LH secretion in females and
182 pulses in males.
183
184 We demonstrate that the GCaMP fiber photometry approach used previously for assessing cell
185 body population activity in this system (Han, Kane et al. 2019, McQuillan, Han et al. 2019) can be
186 adapted to assess activity in neuronal processes. This has been greatly facilitated by the unusual
187 topography of the GnRH neurons in which GnRH neuron projections become highly
188 concentrated in the ventrolateral ARN before passing into the ME. The dendrons in this area

189 display substantial rises in intracellular calcium in response to propagating action potentials as
190 well as to the local application of kisspeptin (Iremonger, Porteous et al. 2017, Liu, Yeo et al.
191 2021). The locations of successful optic fibers immediately above and sometimes lateral to the
192 ARN makes it very unlikely that recordings were made of GnRH neuron activity at the level of
193 their terminals within the ME.
194
195 The GnRH neuron dendrons exhibited clustered high-frequency (approximately 0.01Hz) baseline
196 activity that did not change in profile across 24h in males or throughout the estrous cycle. This
197 would be predicted to give rise to fluctuating, low-level inter-pulse GnRH secretion perhaps
198 compatible with observations made using high-frequency portal sampling in the ewe (Evans,
199 Dahl et al. 1995). High-frequency dopamine release also occurs within the ME between events
200 determining prolactin secretion (Romano, Guillou et al. 2017). The physiological significance of
201 inter-pulse GnRH release at the gonadotroph is unclear (Le Tissier, Campos et al. 2017). For
202 example, the self-priming action of GnRH at the gonadotroph is well characterized for the surge
203 but may also exist at other times of the cycle (Fink 1995). Nevertheless, optogenetic
204 experiments driving GnRH neuron firing at high-frequency burst-like intervals in ovariectomized
205 mice were not found to generate any appreciable change in LH secretion *in vivo* (Campos and
206 Herbison 2014).
207
208 The origin of fluctuating baseline activity in male and female GnRH neuron dendrons is unknown
209 but it is tempting to speculate that it may arise from episodic electrical activity of the GnRH
210 neurons themselves. Brain slice electrophysiological studies have consistently documented
211 repetitive burst firing in GnRH neuron cell bodies (Herbison 2015, Constantin, Moenter et al.
212 2021) and similar patterns of activity were observed in GnRH neurons in anesthetized mice
213 (Constantin, Iremonger et al. 2013). However, there appears to be no mechanism for
214 synchronization between individual GnRH neuron perikarya with dual or multiple recordings of
215 GnRH neuron cell bodies in brain slices never showing any coordinated activity (Constantin,
216 Jasoni et al. 2012, Chen and Moenter 2023). Hence, it is also possible that the rapid baseline
217 activity arises from elsewhere and, for example, the ARN kisspeptin pulse generator is known to
218 exhibit variable inter-synchronization activity (Han, Morris et al. 2023). This baseline pattern of
219 GnRH neuron activity may give rise to fluctuating, low-level inter-pulse GnRH secretion. While
220 not detectable with current LH assays in mice, this is compatible with observations made using
221 high-frequency portal GnRH sampling in the ewe (Evans, Dahl et al. 1995).
222
223 We find abrupt 6-10 min-duration increases in GnRH neuron activity that precede each LH pulse.
224 These events have a dynamic very similar to that of the ARN kisspeptin neuron synchronizations
225 measured using the same technique (Han, Kane et al. 2019, McQuillan, Han et al. 2019).
226 Kisspeptin released from terminals in the ventrolateral ARN operates through volume
227 transmission to rapidly activate and synchronize GnRH neuron dendrons (Iremonger, Porteous
228 et al. 2017, Liu, Yeo et al. 2021). Alongside evidence that pulsatile LH secretion is abolished in

229 the absence of kisspeptin signaling (Liu, Yeo et al. 2021), it is almost certain that the abrupt
230 episodic GnRH neuron activation recorded here arises from up-stream synchronized firing of
231 ARN kisspeptin neurons. What remains curious, however, is that experimentally, the effects of
232 kisspeptin on the dendron are typically prolonged lasting for 10s of minutes *in vitro* (Iremonger,
233 Porteous et al. 2017, Liu, Yeo et al. 2021). Clearly, this is not the case *in vivo* (Fig.6) and it is
234 possible that the termination of GnRH neuron dendron firing to provide a relatively constrained
235 secretory signal involves other local mechanisms such as nitric oxide signaling (Constantin,
236 Reynolds et al. 2021).
237
238 Investigators using a variety of pituitary portal GnRH assays in rodent, sheep and primate
239 models have suggested that GnRH neurons generate the LH surge through either a constant
240 increase in activity or by increasing their normal pulsatile pattern of release (Sarkar, Chiappa et
241 al. 1976, Caraty, Locatelli et al. 1989, Moenter, Brand et al. 1992, Xia, Van Vugt et al. 1992,
242 Clarke 1993, Pau, Berria et al. 1993, Sisk, Richardson et al. 2001). We demonstrate here that,
243 both predictions were correct with GnRH neuron activity changing in a multi-faceted manner
244 comprised of a slowly oscillating baseline increase with superimposed episodic activity.
245 Retrospectively, this is now readily discernable in many of those portal bleeding data (Sarkar,
246 Chiappa et al. 1976, Caraty, Locatelli et al. 1989, Moenter, Brand et al. 1992, Xia, Van Vugt et al.
247 1992, Clarke 1993, Pau, Berria et al. 1993, Sisk, Richardson et al. 2001). The slow oscillating
248 increase in baseline activity observed here is most probably the key event driving the LH surge.
249 It initiates at the time the LH surge begins and has a duration of approximately 12 hours which is
250 very similar to that of GnRH release in the portal system of rats, sheep, and monkeys (Sarkar,
251 Chiappa et al. 1976, Pau, Berria et al. 1993, Karsch, Bowen et al. 1997). The reason for the
252 extremely prolonged period of GnRH neuron activity and secretion that long outlasts the LH
253 surge remains unknown but could be related to sexual behavior (Pfaff 1973, Skinner and Caraty
254 2002). It has been very surprising to find that this gradual increase in activity itself has a slow
255 hourly oscillatory rhythm. While a circadian contribution to the onset of the surge is well
256 established (Tonsfeldt, Mellon et al. 2022), it had not been appreciated that an ultradian rhythm
257 might also exist. It is very likely that the slow increase in GnRH activity recorded here is driven
258 by the preoptic surge generator (Wang, Guo et al. 2020), and it will be interesting in future
259 studies to establish whether ultradian rhythms exist within this circuit and what function they
260 may play in surge generation.

261 The "two compartment model" of GnRH neurons involves independent pulse and surge
262 generators that operate on different parts of the GnRH neuron to bring about pulsatile and
263 surge patterns of gonadotropin secretion (Herbison 2020). We have recently shown that
264 selective suppression of preoptic area kisspeptin expression abolishes the surge generator but
265 has no impact on pulsatile LH secretion (Clarkson, Yip et al. 2023). This model predicts that, on
266 the afternoon of proestrus, the surge generator would operate coincidently with the pulse
267 generator until such time as post-ovulatory progesterone secretion suppresses the pulse
268 generator (Herbison 2020). This model is in accord with our present *in vivo* recordings where we

find abrupt episodic pulse activity to continue on top of the rising phase of the baseline increase until the early hours of estrus when it stops. This highly stereotypical pattern of episodic activity across the surge is identical to that of the ARN kisspeptin pulse generator (McQuillan, Han et al. 2019), further confirming the origin and nature of these abrupt increases in GnRH neuron dendron activity.

An important question is whether pulse generator activity at the time of the surge may contribute to ovulation. While pulse generator events are short in duration, they nevertheless increase the amplitude of total GnRH neuron activity during the rising phase of the surge and presumably also GnRH secretion within the portal system. Mice and sheep with a knockdown of ARN kisspeptin neurons have recently been reported to have reduced LH surge amplitude (Aerts, Griesgraber et al. 2023, Velasco, Franssen et al. 2023) consistent with the concept proposed here that the pulse generator contributes to the LH surge directly through activation of the GnRH neuron dendron. Intriguingly, toxin-induced knockdown of ARN kisspeptin neurons in rats has the opposite effect of increasing LH surge amplitude (Helena, Toporikova et al. 2015, Mittelman-Smith, Krajewski-Hall et al. 2016).

In summary, we provide here the first direct recordings of GnRH neuron activity *in vivo*. These observations demonstrate that alongside a baseline pattern of activity of unknown function, sharp episodic activity underlies pulse generation whereas a slow and prolonged ultradian oscillation on proestrus is responsible for the preovulatory gonadotropin surge. The neurobiological mechanisms underlying this unexpected pattern of surge activity remain to be discovered.

Materials and Methods

Animals

Male and female 129S6Sv/Ev C57BL/6 *Gnrh1*$^{Cre/+}$mice (Yoon, Enquist et al. 2005) crossed on to the Ai162 (TIT2L-GC6s-ICL-tTA2)-D Cre-dependent GCaMP6s line (JAX stock #031562) (Daigle, Madisen et al. 2018) were group-housed in conventional cages with environmental enrichment under conditions of controlled temperature (22±2^{0}C) and lighting (12-hour light/12-hour dark cycle; lights on at 07:00) with *ad libitum* access to food (RM1-P, SDS, UK) and water. All animal experimental protocols were approved by the University of Cambridge Animal Welfare and Ethics Review Body under UK Home Office license, P174441DE.

Stereotaxic implantation of optic fibers

Adult mice were anaesthetized with 2% isoflurane and placed in a stereotaxic frame under buprenorphine (0.05mg/kg, s.c.) and meloxicam (5 mg/kg, s.c.) analgesia. Dexamethasone (10 mg/kg, s.c.) was used to prevent cranial swelling. A single 400-μm diameter optic fiber (0.48 NA, Doric lenses, QC, Canada) was implanted into the brain with the tip placed immediately above

307 the dorsomedial part of ARN (A-P to bregma, -2.0mm; D-V 5.9mm, M-L ±0.2mm to sagittal
308 sinus). Following one week of surgery, all animals were handled daily and habituated to a
309 photometry recording setup for at least three weeks.
310
311 *GCaMP6 fiber photometry and blood sampling*
312 Over a period of 4 to 12 weeks after surgery, fiber photometry experiments were undertaken to
313 record GCaMP fluorescence signal in freely behaving mice for 6 or 24 h periods using previously
314 described methodology (Han, Kane et al. 2019, Han, Morris et al. 2023). This included a custom-
315 built photometry system using Doric components (Doric Lenses, QC, Canada) and National
316 Instrument data acquisition board (TX, USA) based on a previous design (Lerner, Shilyansky et al.
317 2015). Blue (465-490 nm) and violet (405 nm) LED lights were sinusoidally modulated at
318 frequencies of 531 and 211 Hz respectively and were focused onto a single fiber optic connected
319 to the mouse. The light intensity at the tip of the fiber was 30-80 microwatts. Emitted
320 fluorescence signal from the brain was collected via the same fiber, passed through a 500-550
321 nm emission filter and focused onto a fluorescence detector (Doric, QC, Canada). The emissions
322 were collected at 10 Hz and the two GCaMP6 emissions were recovered by demodulating the
323 465-490 nm signals (calcium-dependent) and 405 nm (calcium-independent) signals. Signals
324 were either recorded in a continuous mode or a scheduled 5s on/10s off mode.
325 Analysis was performed in MATLAB with the subtraction of 405 signal from 465-490 signal to
326 extract the calcium-dependent signal followed by an exponential fit algorithm used to correct
327 for baseline shift. The signal was converted to $\Delta F/F$ (%) values using the equation $\Delta F/F=(F_{recorded}-$
328 $F_{baseline})/ F_{baseline}) \times 100$. The Findpeaks algorithm was used to detect dSEs, and the duration and
329 the time of SE to the half width full maximum was determined. For deconvolution of signals
330 from 24-h proestrus recordings, the movmean algorithm was used to extract 30-min rolling
331 average followed by separating dSE signals (-60 to 360 s around each peak) to visualize the
332 remaining low amplitude 'residual' signal. A threshold of 5% above baseline was used to extract
333 the residual signal. Residual signals with peaks occurring > 420s from the preceding peak were
334 considered to represent separate clusters.
335
336 To examine the relationship between calcium episodes with LH pulses, freely behaving mice
337 were attached to the fiber photometry system, and 4-μL blood samples were obtained every 5
338 to 10 minutes from the tail tip over a period of 120 to 240 minutes. To assess the relationship
339 between the long calcium increment during proestrus evening and the LH surge, female mice
340 were attached to the fiber photometry system in the morning of proestrus and blood samples
341 (3-μL) collected every 3 hours for 18 hours until the morning of estrus. Levels of LH were
342 measured by in-house LH ELISA (Steyn, Wan et al. 2013) with an assay sensitivity of 0.04 ng/mL
343 and intra-assay coefficient of variation of 8.2%.
344
345 *Immunohistochemistry*

Adult GnRH-Cre,GCaMP6s mice were given a lethal overdose of pentobarbital (3mg/100μL, i.p.) and perfused transcardially with 4% paraformaldehyde. Brains were processed for dual GFP and GnRH immunofluorescence. For GFP immunostaining, anti-chicken GFP (1:5000, Aves Lab) was used followed by AlexaFluor 488-conjugated goat-anti-chicken (1:1000). For GnRH cell body immunostaining, GA2 guinea pig anti-GnRH antisera (1:3000, gift from G.Anderson, New Zealand) was used in combination with AlexaFluor 647-conjugated goat anti-guinea pig immunoglobulin (1:500, Thermo Fisher Scientific, USA). For GnRH dendron immunostaining, rabbit anti-GnRH (1:20,000, LR1, gift of R.Benoit, Montreal) antisera was used followed by biotinylated goat anti-rabbit immunoglobulin (1:1000, Jackson Immunoresearch) and AlexaFluor 568-conjugated Streptavidin (1:400, Thermo Fisher Scientific, USA). Imaging was performed using a Leica SP8 Laser Scanning Confocal Microscope (Leica Microsystems) at the Cambridge Advanced Imaging Center and analyzed using ImageJ.

Statistical Analysis

All statistical analyses were performed in Prism 10 (GraphPad software Inc.). All values given in this study are mean ± SEM, and significance is defined as $P < 0.05$* or $P < 0.01$**. For inter-peak interval analysis in females across the estrous cycle and the residual cluster activity analysis, Kruskal Wallis ANOVA followed by Dunn's post-hoc tests was used.

Acknowledgments

This work was supported by the Wellcome Trust (212242/Z/18/Z). JCK received a Doc.Mobility Fellowship (P1ZHP1_184166) from the Swiss National Science Foundataion. We thank Ms. Maria Pardo-Navarro for technical assistance. For the purpose of open access, the author has applied a Creative Commons Attribution (CC BY) license to any Author Accepted Manuscript version arising from this submission.

Author Contributions: SYH, SHY and ZZ undertook investigations; SYH, SHY and JCK performed analysis; SYH and AEH designed experiments and wrote the manuscript: AEH generated funding.

Figure Legends

Figure 1. *GCaMP expression in GnRH neurons*. (A) Photomicrographs at the level of organum vasculosm of the laminae terminalis (OVLT) showing GFP immunofluorescence representing GCaMP6 (green), GnRH (purple) and merged channels showing double labelled cells (white). (B) Photomicrographs of four mice at the level of arcuate nucleus showing the location of the end of the optic fiber (dotted line) in relation to GnRH neuron dendrons labeled with GnRH (red), GFP representing GCaMP6 (green) and merged channels showing double labelled (yellow). 3V, third ventricle.

385 **Figure 2.** *GnRH neuron dendron activity in male mice*. (A) A representative example of 24-h
386 GCaMP6 photometry recording showing abrupt dendron synchronized episodes (dSEs) occurring
387 on lower amplitude baseline activity in a male mouse. Below, expanded view of the trace
388 indicated by the horizontal line. (B) Example of 8-h GCaMP6 photometry recording in a male
389 mouse with a misplaced fiber optic. All recorded signals are under 3% of baseline. Below,
390 expanded view of the trace indicated by the horizontal line. (C) Average high-resolution profile
391 of an dSE in male mice (N=7 mice) showing a rapid onset followed by a gradual decrease back to
392 baseline. 'a' and 'b' give values at full-width half maximum (FWHM). (D) Inter-peak intervals
393 combined from all recordings (n= 96 dSEs) displayed as a percentage of all intervals occurring in
394 5-min bins. (E) Representative example showing the relationship of dSEs (black) to pulsatile LH
395 secretion (red). (F) Normalized increase in LH plotted against the dSEs, with the time 0 being the
396 peak of dSE.

397 **Figure 3.** *GnRH neuron dendron activity in female mice*. (A) Representative example of 6-h
398 GCaMP6 photometry recording from female mice in (i) metestrus, (ii) diestrus, (iii) proestrus,
399 and (iv) estrus. (B) Average high-resolution profile of dSEs in female mice showing a rapid onset
400 followed by a gradual decrease in the signal. 'a' and 'b' show the values at full-width half
401 maximum (FWHM). (C) Histograms showing inter-peak intervals of dSEs across the estrous cycle.
402 M = metestrus, D = diestrus, P = proestrus E = estrus. *P<0.05, **P<0.01, Kruskal Wallis followed
403 by Dunn's post-hoc test. (D) Inter-peak intervals combined from all recordings (n= 245 dSEs)
404 across metestrus, diestrus, proestrus and estrus displayed as a percentage of all intervals
405 occurring in 5-min bins. (E) A representative example showing the relationship of dSEs (black) to
406 pulsatile LH secretion (red). (F) Normalized increase in LH plotted against the dSEs, with the time
407 0 being the peak of dSE.

408 **Figure 4.** *Baseline high-frequency cluster activity of GnRH neuron dendrons in male and female*
409 *mice.* Representative 4-h GCaMP recordings in (A) two male mice and (B) a female mouse across
410 the different stages of the estrous cycle showing high frequency baseline activity and larger
411 increases in calcium activity representing dendron synchronization episodes (dSEs) indicated by
412 red asterisks. The peaks of dSEs reaching >30% dFF were cut off to optimize the display of the
413 low amplitude activities. Histograms showing the duration (C) and the intra-cluster frequency
414 (D) of the baseline activity in male and female mice. No significance was found across the
415 groups. M= metestrus, D = diestrus, P = proestrus, E= estrus.

416 **Figure 5**. *Slow oscillating increases in calcium activity on the afternoon of proestrus in female*
417 *mice*. (A) Examples of 21-h GCaMP recordings from four proestrous female mice. Note the
418 prolonged (>10h) gradual oscillating increase in calcium signal beginning on the afternoon of
419 proestrus. The sharp dSEs continue until approximately the plateau phase of the increased
420 baseline at which time they stop or slow. (B) A representative example showing the relationship
421 of the slow increase in baseline calcium activity (black) with LH surge (red). Note that the rise in

LH occurs in alongside the initial rise in calcium activity but returns to baseline several hours before the calcium signal.

Figure 6. *Deconvolution of the GCaMP signal across the proestrous surge reveals multimodal activity patterns of GnRH neuron dendron*. (A-B) Representative examples of 24-h photometry recordings from two female mice starting at proestrus showing (i) the original recording, (ii) 30-min rolling average highlighting the LH surge signal (red), (iii) the LH surge signal subtracted from the original recording, displaying the dSEs (blue), and (iv) the residual baseline signal (pink) after subtracting both the surge and pulse profiles.

References

Aerts, E. G., M. J. Griesgraber, S. L. Shuping, E. C. Bowdridge, S. L. Hardy, R. L. Goodman, C. C. Nestor and S. M. Hileman (2023). "The effect of NK3-Saporin injection within the arcuate nucleus on puberty, the LH surge, and the response to Senktide in female sheep." Biol Reprod.

Amoss, M., R. Burges, R. Blackwell, W. Vale, R. Fellows and R. Guillemin (1971). "Purification, amino acid composition and N-terminus of the hypothalamic luteinizing hormone releasing hormone factor (LRF) of ovine origin." Biochemical Biophysical Research Communication. **44**: 205-210.

Barry, J. (1979). "Immunohistochemistry of luteinizing hormone-releasing hormone-producing neurons of the vertebrates." Int Rev Cytol **60**: 179-221.

Campos, P. and A. E. Herbison (2014). "Optogenetic activation of GnRH neurons reveals minimal requirements for pulsatile luteinizing hormone secretion." Proc Natl Acad Sci U S A **111**(51): 18387-18392.

Caraty, A. and A. Locatelli (1988). "Effect of time after castration on secretion of LHRH and LH in the ram." J Reprod Fertil **82**(1): 263-269.

Caraty, A., A. Locatelli and G. B. Martin (1989). "Biphasic response in the secretion of gonadotrophin-releasing hormone in ovariectomized ewes injected with oestradiol." Journal of Endocrinology **123**: 375-382.

Chen, X. and S. M. Moenter (2023). "Gonadal Feedback Alters the Relationship between Action Potentials and Hormone Release in Gonadotropin-Releasing Hormone Neurons in Male Mice." J Neurosci **43**(40): 6717-6730.

Clarke, I. J. (1993). "Variable patterns of gonadotropin-releasing hormone secretion during the estrogen-induced luteinizing hormone surge in ovariectomized ewes." Endocrinology **133**: 1624-1632.

Clarke, I. J. (2018). Generation of the GnRH surge and LH surge by the positive feedback effect of estrogen. The GnRH neuron and its control. A. E. Herbison and T. M. Plant, John Wiley & Sons**:** 325-356.

Clarke, I. J. and J. T. Cummins (1982). "The temporal relationship between gonadotropin releasing hormone (GnRH) and luteinizing hormone (LH) secretion in ovariectomized ewes." Endocrinology **111**(5): 1737-1739.

462 Clarkson, J., S. H. Yip, R. Porteous, A. Kauff, A. K. Heather and A. E. Herbison (2023). "CRISPR-
463 Cas9 knockdown of ESR1 in preoptic GABA-kisspeptin neurons suppresses the preovulatory
464 surge and estrous cycles in female mice." eLife.90959.1

465 Constantin, S. (2017). "Progress and Challenges in the Search for the Mechanisms of Pulsatile
466 Gonadotropin-Releasing Hormone Secretion." Front Endocrinol (Lausanne) **8**: 180.
467 Constantin, S., K. J. Iremonger and A. E. Herbison (2013). "In vivo recordings of GnRH neuron
468 firing reveal heterogeneity and dependence upon GABAA receptor signaling." J Neurosci **33**(22):
469 9394-9401.
470 Constantin, S., C. Jasoni, N. Romano, K. Lee and A. E. Herbison (2012). "Understanding calcium
471 homeostasis in postnatal gonadotropin-releasing hormone neurons using cell-specific Pericam
472 transgenics." Cell Calcium **51**(3-4): 267-276.
473 Constantin, S., S. M. Moenter and R. Piet (2021). "The electrophysiologic properties of
474 gonadotropin-releasing hormone neurons." J Neuroendocrinol: e13073.
475 Constantin, S., D. Reynolds, A. Oh, K. Pizano and S. Wray (2021). "Nitric oxide resets kisspeptin-
476 excited GnRH neurons via PIP2 replenishment." PNAS **118**: e2012339118.
477 Daigle, T. L., L. Madisen, T. A. Hage, M. T. Valley, U. Knoblich, R. S. Larsen, M. M. Takeno, L.
478 Huang, H. Gu, R. Larsen, M. Mills, A. Bosma-Moody, L. A. Siverts, M. Walker, L. T. Graybuck, Z.
479 Yao, O. Fong, T. N. Nguyen, E. Garren, G. H. Lenz, M. Chavarha, J. Pendergraft, J. Harrington, K. E.
480 Hirokawa, J. A. Harris, P. R. Nicovich, M. J. McGraw, D. R. Ollerenshaw, K. A. Smith, C. A. Baker, J.
481 T. Ting, S. M. Sunkin, J. Lecoq, M. Z. Lin, E. S. Boyden, G. J. Murphy, N. M. da Costa, J. Waters, L.
482 Li, B. Tasic and H. Zeng (2018). "A Suite of Transgenic Driver and Reporter Mouse Lines with
483 Enhanced Brain-Cell-Type Targeting and Functionality." Cell **174**(2): 465-480 e422.
484 Evans, N. P., G. E. Dahl, D. Mauger and F. J. Karsch (1995). "Estradiol induces both qualitative
485 and quantitative changes in the pattern of gonadotropin-releasing hormone secretion during
486 the presurge period in the ewe." Endocrinology **136**: 1603-1609.
487 Fink, G. (1995). "The self-priming effect of LHRH: a unique servomechanism and possible cellular
488 model for memory." Front Neuroendocrinol **16**(2): 183-190.
489 Fink, G. (2015). "60 YEARS OF NEUROENDOCRINOLOGY: MEMOIR: Harris' neuroendocrine
490 revolution: of portal vessels and self-priming." J Endocrinol **226**(2): T13-24.
491 Goodman, R. L., A. E. Herbison, M. N. Lehman and V. M. Navarro (2022). "Neuroendocrine
492 control of gonadotropin-releasing hormone: Pulsatile and surge modes of secretion." J
493 Neuroendocrinol **34**(5): e13094.
494 Han, S. Y., G. Kane, I. Cheong and A. E. Herbison (2019). "Characterization of GnRH Pulse
495 Generator Activity in Male Mice Using GCaMP Fiber Photometry." Endocrinology **160**(3): 557-
496 567.
497 Han, S. Y., P. G. Morris, J. C. Kim, S. Guru, M. Pardo-Navarro, S. H. Yeo, H. J. McQuillan and A. E.
498 Herbison (2023). "Mechanism of kisspeptin neuron synchronization for pulsatile hormone
499 secretion in male mice." Cell Rep **42**(1): 111914.
500 Harris, G. W. (1955). Neural control of the pituitary gland. London, Edward Arnold.
501 Helena, C. V., N. Toporikova, B. Kalil, A. M. Stathopoulos, V. V. Pogrebna, R. O. Carolino, J. A.
502 Anselmo-Franci and R. Bertram (2015). "KNDy Neurons Modulate the Magnitude of the Steroid-
503 Induced Luteinizing Hormone Surges in Ovariectomized Rats." Endocrinology **156**(11): 4200-
504 4213.
505 Herbison, A. E. (2015). Physiology of the adult GnRH neuronal network. Knobil and Neill's
506 Physiology of Reproduction. T. M. Plant and A. J. Zeleznik, Academic Press. **1:** 399-467.

507 Herbison, A. E. (2018). "The gonadotropin-releasing hormone pulse generator." Endocrinology
508 **159**(11): 3723-3736.
509 Herbison, A. E. (2020). "A simple model of estrous cycle negative and positive feedback
510 regulation of GnRH secretion." Front Neuroendocrinol **57**: 100837.
511 Herbison, A. E. (2021). "The dendron and episodic neuropeptide release." J Neuroendocrinol:
512 e13024.
513 Iremonger, K. J., R. Porteous and A. E. Herbison (2017). "Spike and neuropeptide-dependent
514 mechanisms control GnRH neuron nerve terminal Ca2+ over diverse time scales." J Neurosci
515 **37**(12): 3342-3351.
516 Karsch, F. J., J. M. Bowen, A. Caraty, N. P. Evans and S. M. Moenter (1997). "Gonadotropin-
517 releasing hormone requirements for ovulation." Biol Reprod **56**: 303-309.
518 Le Tissier, P., P. Campos, C. Lafont, N. Romano, D. J. Hodson and P. Mollard (2017). "An updated
519 view of hypothalamic-vascular-pituitary unit function and plasticity." Nat Rev Endocrinol **13**(5):
520 257-267.
521 Lerner, T. N., C. Shilyansky, T. J. Davidson, K. E. Evans, K. T. Beier, K. A. Zalocusky, A. K. Crow, R.
522 C. Malenka, L. Luo, R. Tomer and K. Deisseroth (2015). "Intact-Brain Analyses Reveal Distinct
523 Information Carried by SNc Dopamine Subcircuits." Cell **162**(3): 635-647.
524 Liu, X., S. H. Yeo, H. J. McQuillan, M. K. Herde, S. Hessler, I. Cheong, R. Porteous and A. E.
525 Herbison (2021). "Highly redundant neuropeptide volume co-transmission underlying episodic
526 activation of the GnRH neuron dendron." Elife **10**.
527 McQuillan, H. J., S. Y. Han, I. Cheong and A. E. Herbison (2019). "GnRH Pulse Generator Activity
528 Across the Estrous Cycle of Female Mice." Endocrinology **160**(6): 1480-1491.
529 Mittelman-Smith, M. A., S. J. Krajewski-Hall, N. T. McMullen and N. E. Rance (2016). "Ablation of
530 KNDy Neurons Results in Hypogonadotropic Hypogonadism and Amplifies the Steroid-Induced
531 LH Surge in Female Rats." Endocrinology **157**(5): 2015-2027.
532 Moenter, S. M., R. C. Brand and F. J. Karsch (1992). "Dynamics of gonadotropin-releasing
533 hormone (GnRH) secretion during the GnRH surge: insights into the mechanism of GnRH surge
534 induction." Endocrinology **130**(5): 2978-2984.
535 Pau, K. F., M. Berria, D. L. Hess and H. G. Spies (1993). "Preovulatory gonadotropin-releasing
536 hormone surge in ovarian-intact rhesus macaques." Endocrinology **133**: 1650-1656.
537 Pfaff, D. W. (1973). "Luteinizing hormone-releasing factor potentiates lordosis behavior in
538 hypophysectomized ovariectomized female rats." Science **182**(117): 1148-1149.
539 Romano, N., A. Guillou, D. J. Hodson, A. O. Martin and P. Mollard (2017). "Multiple-scale
540 neuroendocrine signals connect brain and pituitary hormone rhythms." Proc Natl Acad Sci U S A
541 **114**(9): 2379-2382.
542 Sarkar, D. K., S. A. Chiappa, G. Fink and N. M. Sherwood (1976). "Gonadotropin-releasing
543 hormone surge in pro-oestrous rats." Nature **264**: 461-463.
544 Schally, A. V., A. Arimura, Y. Baba, R. M. Nair, H. Matsuo, T. W. Redding and L. Debeljuk (1971).
545 "Isolation and properties of the FSH and LH-releasing hormone." Biochem Biophys Res Commun
546 **43**(2): 393-399.
547 Sisk, C. L., H. N. Richardson, P. E. Chappell and J. E. Levine (2001). "In vivo gonadotropin-
548 releasing hormone secretion in female rats during peripubertal development and on proestrus."
549 Endocrinology **142**(7): 2929-2936.
550 Skinner, D. C. and A. Caraty (2002). "Measurement and possible function of GnRH in
551 cerebrospinal fluid in ewes." Reprod Suppl **59**: 25-39.

552 Steyn, F. J., Y. Wan, J. Clarkson, J. D. Veldhuis, A. E. Herbison and C. Chen (2013). "Development
553 of a methodology for and assessment of pulsatile luteinizing hormone secretion in juvenile and
554 adult male mice." Endocrinology **154**(12): 4939-4945.
555 Tonsfeldt, K. J., P. L. Mellon and H. M. Hoffmann (2022). "Circadian Rhythms in the Neuronal
556 Network Timing the Luteinizing Hormone Surge." Endocrinology **163**(2).
557 Velasco, I., D. Franssen, S. Daza-Duenas, K. Skrapits, S. Takacs, E. Torres, E. Rodriguez-Vazquez,
558 M. Ruiz-Cruz, S. Leon, K. Kukoricza, F. P. Zhang, S. Ruohonen, D. Luque-Cordoba, F. Priego-
559 Capote, F. Gaytan, F. Ruiz-Pino, E. Hrabovszky, M. Poutanen, M. J. Vazquez and M. Tena-
560 Sempere (2023). "Dissecting the KNDy hypothesis: KNDy neuron-derived kisspeptins are
561 dispensable for puberty but essential for preserved female fertility and gonadotropin
562 pulsatility." Metabolism **144**: 155556.
563 Wang, L., W. Guo, X. Shen, S. Yeo, H. Long, Z. Wang, Q. Lyu, A. E. Herbison and Y. Kuang (2020).
564 "Different dendritic domains of the GnRH neuron underlie the pulse and surge modes of GnRH
565 secretion in female mice." Elife **9**.
566 Xia, L., D. Van Vugt, E. J. Alston, J. Luckhaus and M. Ferin (1992). "A surge of gonadotropin-
567 releasing hormone accompanies the estradiol-induced gonadotropin surge in the rhesus
568 monkey." Endocrinology **131**: 2812-2820.
569 Yoon, H., L. W. Enquist and C. Dulac (2005). "Olfactory inputs to hypothalamic neurons
570 controlling reproduction and fertility." Cell **123**(4): 669-682.

571

572

573

574

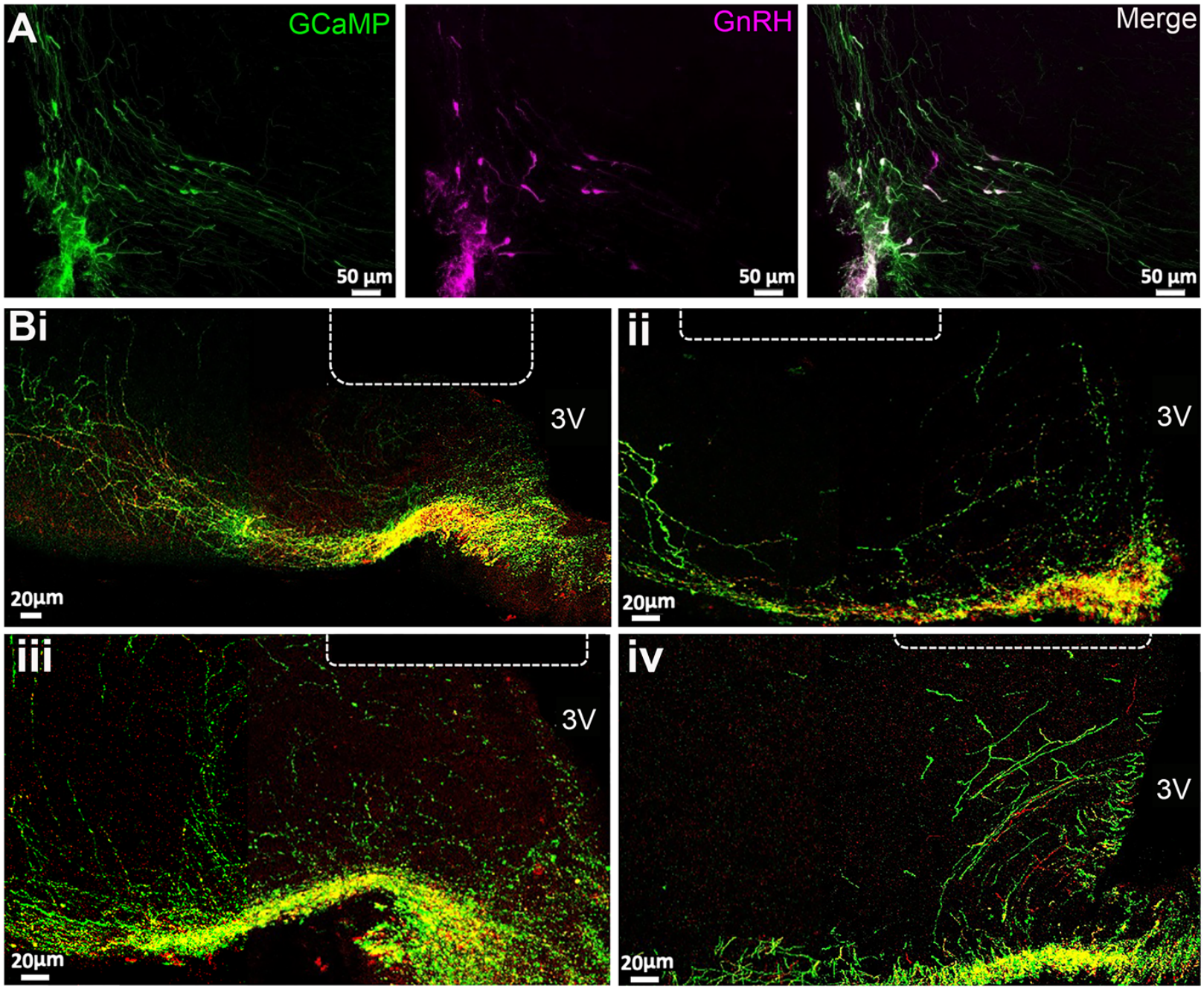
A
GCaMP
50 µm
GnRH
50 µm
Merge
50 µm
Bi
3V
20µm
ii
3V
20µm
iii
3V
20µm
iv
3V
20µm

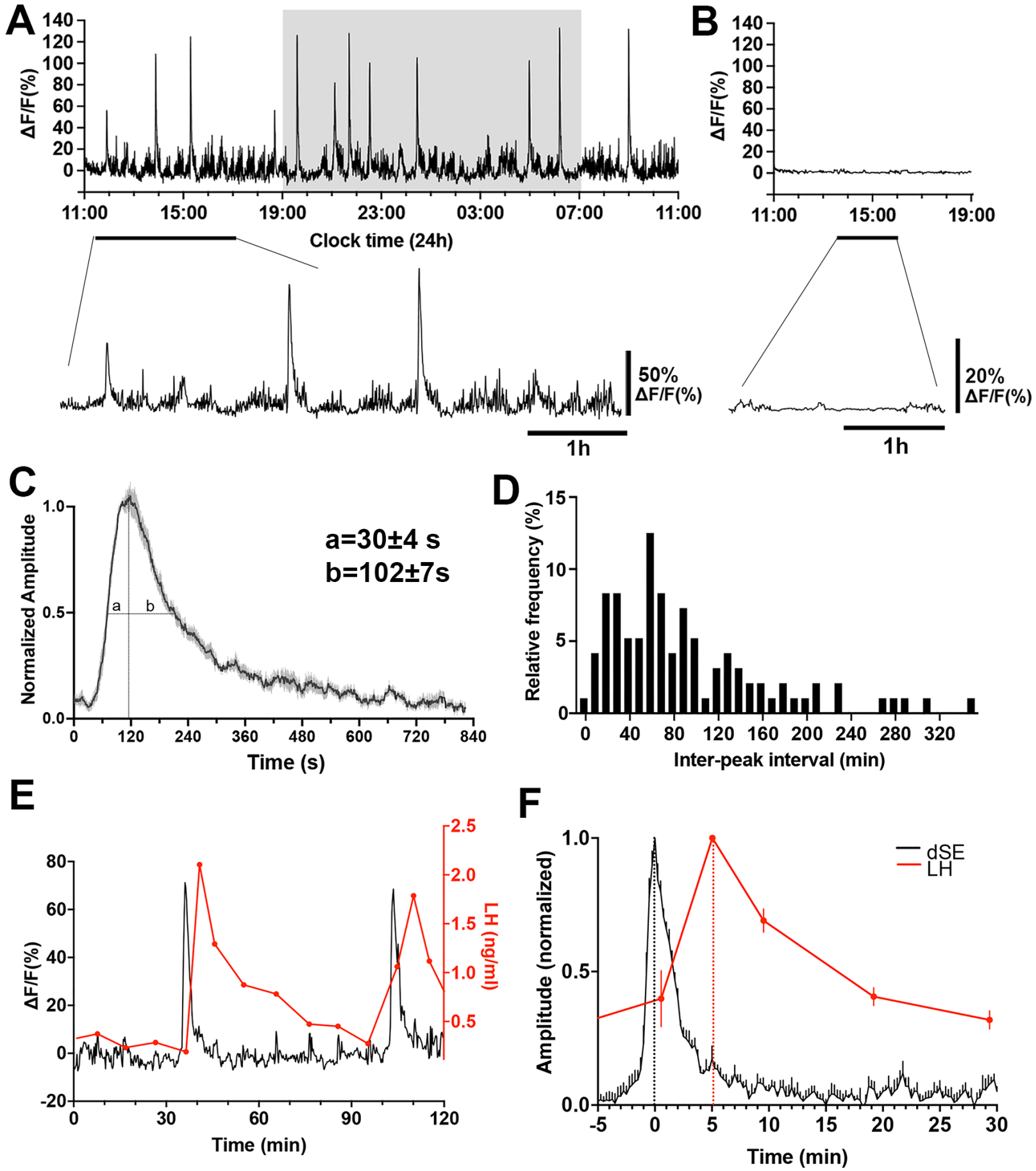
A
ΔF/F(%)
Clock time (24h)
50% ΔF/F(%)
1h
B
ΔF/F(%)
20% ΔF/F(%)
1h
C
Normalized Amplitude
a=30±4 s
b=102±7s
Time (s)
D
Relative frequency (%)
Inter-peak interval (min)
E
ΔF/F(%)
LH (ng/ml)
Time (min)
F
Amplitude (normalized)
dSE
LH
Time (min)

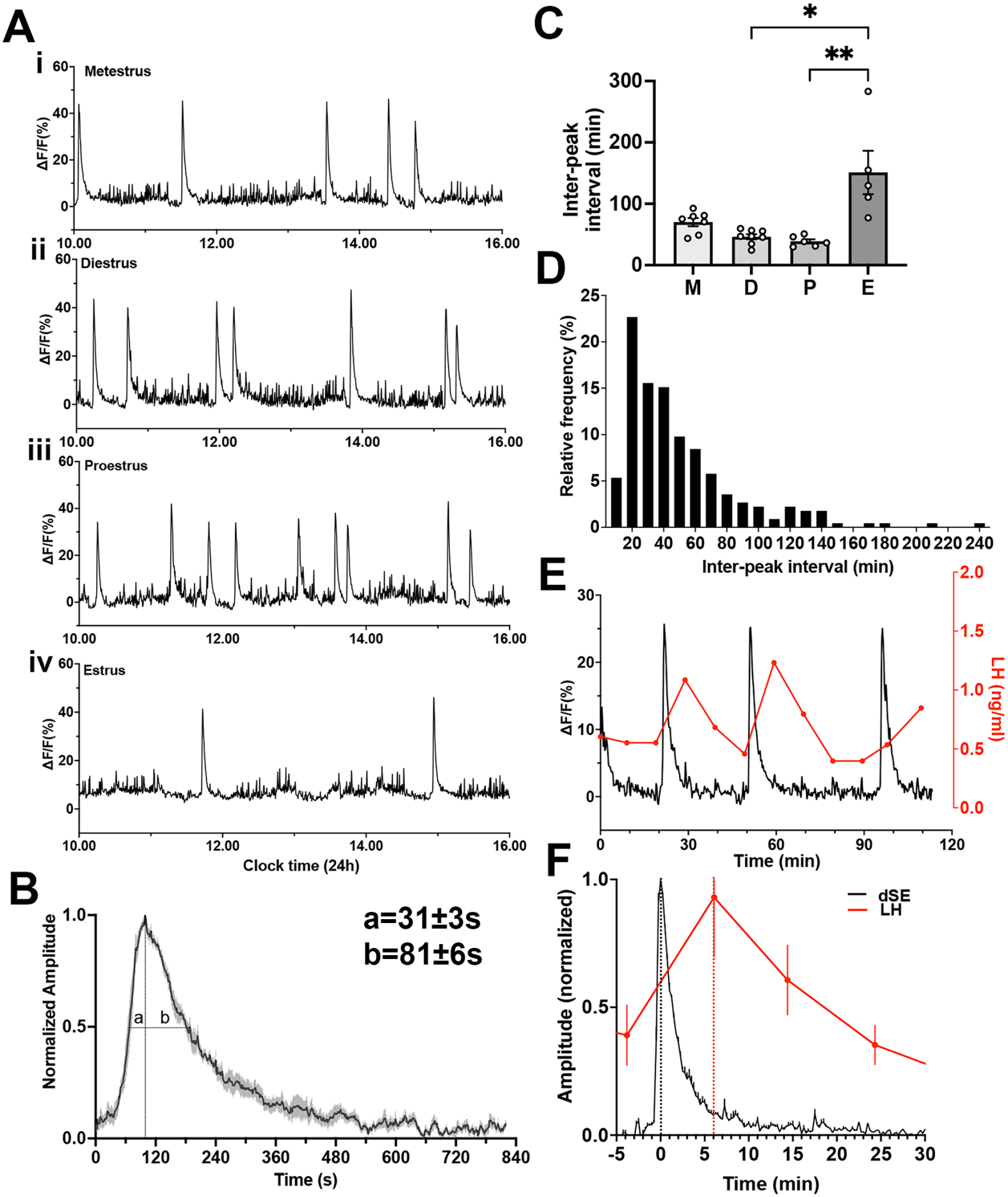
A
i
Metestrus
ΔF/F(%)
ii
Diestrus
iii
Proestrus
iv
Estrus
Clock time (24h)
B
a=31±3s
b=81±6s
Normalized Amplitude
Time (s)
C
Inter-peak interval (min)
M
D
P
E
D
Relative frequency (%)
Inter-peak interval (min)
E
ΔF/F(%)
LH (ng/ml)
Time (min)
F
dSE
LH
Amplitude (normalized)
Time (min)

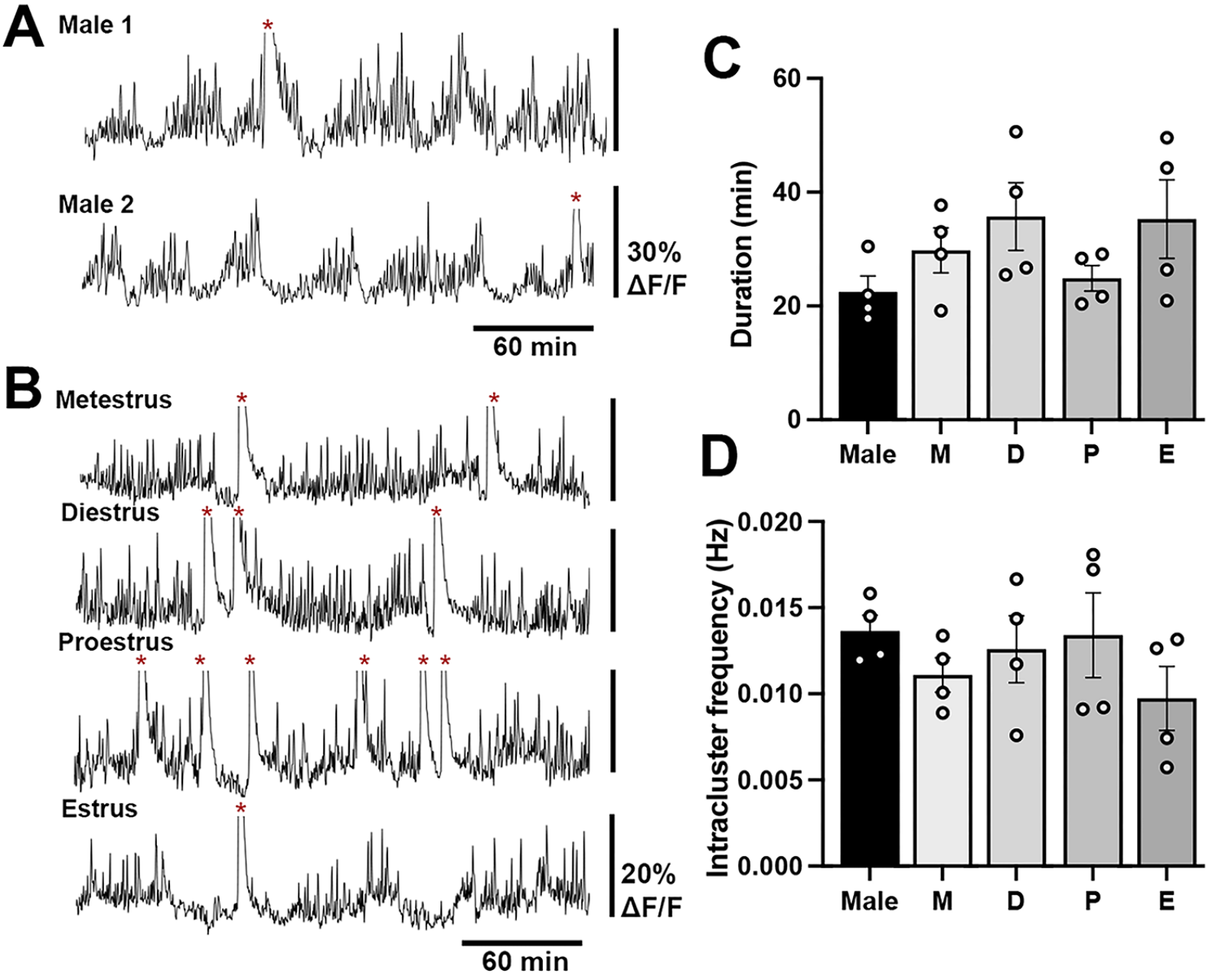
A
Male 1
Male 2
30%
ΔF/F
60 min
B
Metestrus
Diestrus
Proestrus
Estrus
20%
ΔF/F
60 min
C
Duration (min)
60
40
20
0
Male
M
D
P
E
D
Intracluster frequency (Hz)
0.020
0.015
0.010
0.005
0.000
Male
M
D
P
E

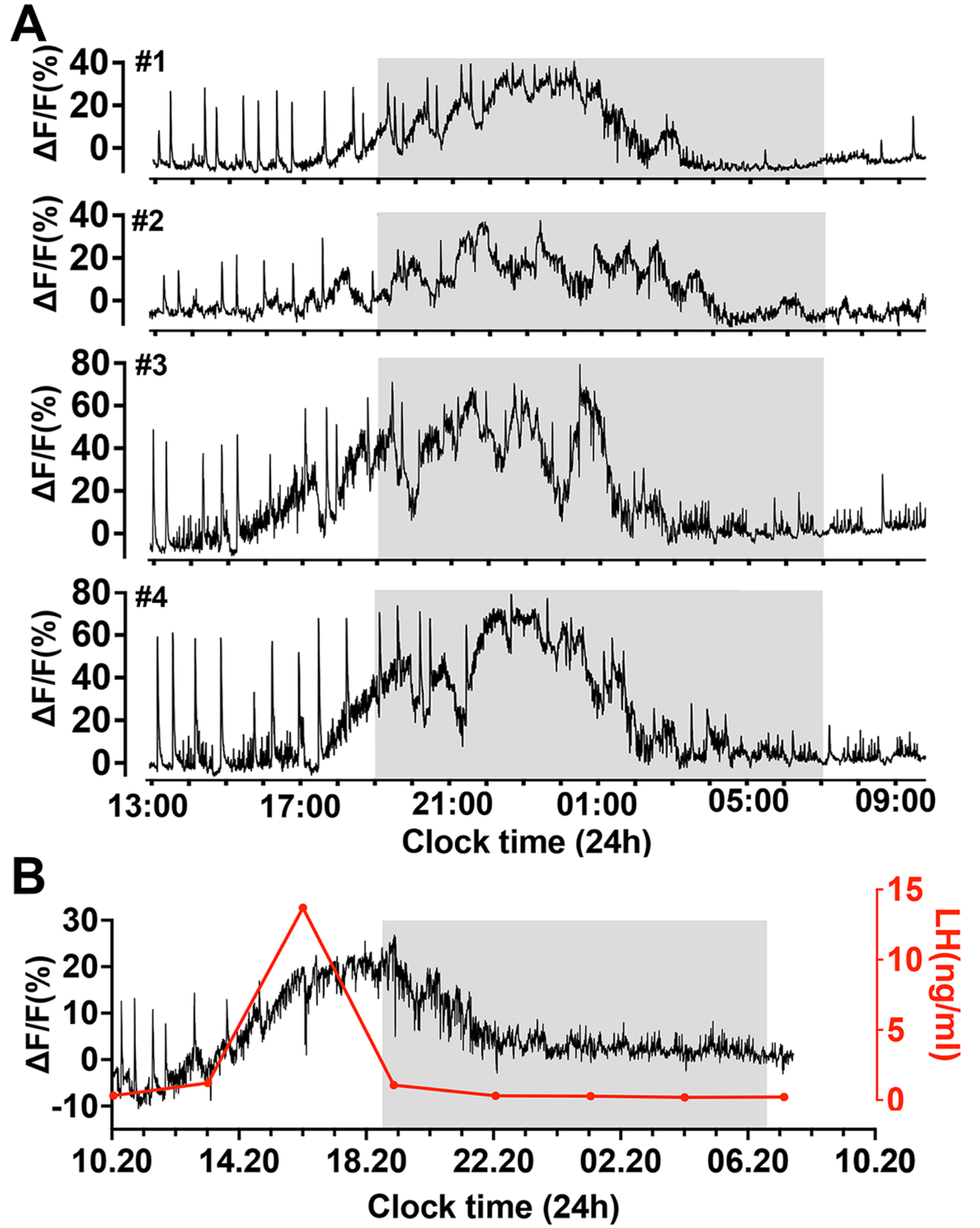
A
#1
#2
#3
#4
ΔF/F(%)
40
20
0
80
60
13:00
17:00
21:00
01:00
05:00
09:00
Clock time (24h)
B
30
10
-10
LH(ng/ml)
15
5
10.20
14.20
18.20
22.20
02.20
06.20
Clock time (24h)

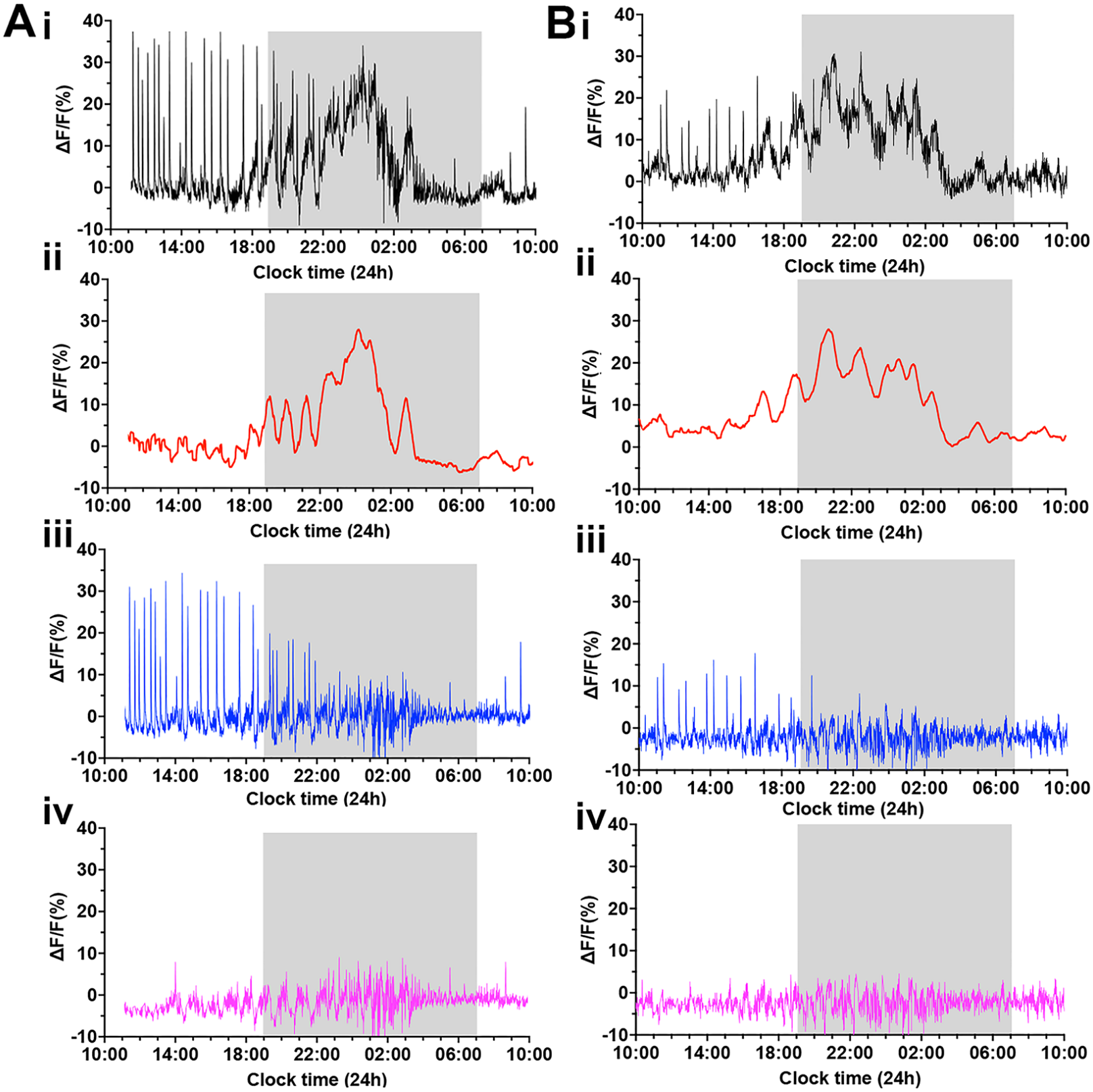
Ai
Bi
ii
iii
iv
ΔF/F(%)
40
30
20
10
0
-10
10:00
14:00
18:00
22:00
02:00
06:00
10:00
Clock time (24h)